Accepted Manuscript

Geometric constraints on quadratic Bézier curves using minimal length and energy

Young Joon Ahn, Christoph Hoffmann, Paul Rosen

PII: S0377-0427(13)00349-X
DOI: http://dx.doi.org/10.1016/j.cam.2013.07.005
Reference: CAM 9231

To appear in: *Journal of Computational and Applied Mathematics*

Received date: 10 November 2011
Revised date: 4 July 2013

Please cite this article as: Y.J. Ahn, C. Hoffmann, P. Rosen, Geometric constraints on quadratic Bézier curves using minimal length and energy, *Journal of Computational and Applied Mathematics* (2013), http://dx.doi.org/10.1016/j.cam.2013.07.005

Geometric constraints on quadratic Bézier curves using minimal length and energy

Young Joon Ahn [a], Christoph Hoffmann [b] and Paul Rosen [c]

[a] *Department of Mathematics Education, Chosun University, Gwangju, 501–759, South Korea*

[b] *Department of Computer Science, Purdue University, West Lafayette, IN 47907, USA*

[c] *Department of Computer Science, University of Utah, Salt Lake City, UT 84112, USA*

Abstract

This paper derives expressions for the arc length and the bending energy of quadratic Bézier curves. The formulae are in terms of the control point coordinates. For fixed start and end points of the Bézier curve, the locus of the middle control point is analyzed for curves of fixed arc length or bending energy. In the case of arc length this locus is convex. For bending energy it is not. Given a line or a circle and fixed end points, the locus of the middle control point is determined for those curves that are tangent to a given line or circle. For line tangency, this locus is a parallel line. In the case of the circle, the locus can be classified into one of six major types. In some of these cases, the locus contains circular arcs. These results are then used to implement fast algorithms that construct quadratic Bézier curves tangent to a given line or circle, with given end points, that minimize bending energy or arc length.

Key words: quadratic Bézier curve; geometric constraint solving; arc length; bending energy; minimum arc length; minimum bending energy; optimization; GPU implementation; circle transition.

1 Introduction

We consider the following set of problems:

> Given end points $\mathbf{b}_0$ and $\mathbf{b}_2$ of a quadratic Bézier curve $\mathbf{q}(t)$, and a line or circle to which the curve should be tangent. Find a curve that has minimum arc length or minimum bending energy.

Our study is a continuation of work that seeks to use free-form curves in geometric constraint problems [1]. Curves that minimize bending energy or have minimum arc length are sometimes considered to be fair in CAGD [4,5,11,20,22,32]. Finding such curves subject to geometric constraints offers the ability to find curves that are to have prescribed clearance from points, circles or straight-line borders, and so has applications in mechanical CAD[6] as well as in motion planning. For instance, Moll and Kavraki [23] consider motion planning for elastic objects. Roughly speaking, a flexible rectangular object is moved past a set of obstacles and is flexing along the path as required for the passage. They determine the required flexing numerically using a bending energy functional.

We address the problem of finding minimum length or minimum energy curves with tangency constraints by deriving, for these curves, analytical expressions for arc length and bending energy. We then solve the constraint problem by utilizing the high parallelism of the GPU. The tangency constraints are solved using a locus method. For example, given the points $\mathbf{b}_0$ and $\mathbf{b}_2$ and the tangent line T, the locus of the middle control point $\mathbf{b}_1$ of all quadratic Bézier curves tangent to T is a parallel to T at a distance easily determined from the distances of $\mathbf{b}_0$ and $\mathbf{b}_2$ from T. We also prove that the solution of the minimum length tangency problem is unique.

Prior work on finding Bézier curves with minimum arc length as constraint includes the following: [21] gives an analytic formula for the arc length of quadratic Bézier curves. This is a well-known result. Cubic Bézier curves, on the other hand, do not have a closed form analytic arc length expression in general, and require approximation [12,13]. However, finding cubic Hermite interpolants subject to minimum arc length has been done using iteration; e.g., [7].

Prior work on minimum energy curves includes [9] who develops analytic formulae for the bending energy of Pythagorean Hodograph curves of degree 3 and 5. [19] devises tools to find minimum energy splines under prescribed end tangency conditions. The curves are approximated from first principles and are not Bézier curves. [8] considers the Hermite interpolation problem with minimal energy curves. The curves are integrated from piecewise polynomial curvature functions. We are not aware of a prior, closed-form expression for bending energy of quadratic Bézier curves; however, the derivation of such a formula is elementary and is sketched for completeness.

We also consider the *Circle Transition Problem* that asks to connect tangentially two given circles with a Bézier curve. Several variants of this problem have been studied, including connecting the circles with composite cubic spiral Bézier curves[15,27]; with PH quintic spiral curves[14,17,28,30]; with fair or single cubic curves[16,29]; and with Bézier-like cubic functions[31]. We solve

the circle transition problem using quadratic Bézier curve, or equivalently parabolic arc, which minimizes the linear combination of length and bending energy. This result has a merit. The parabolic arc has rational offset of degree six[2,3,10], so its offset can be obtained instantaneously in the form of rational Bézier curve.

In the remainder of this paper, we introduce notation and preliminaries in Section 2. Section 3 analyzes the locus of the middle control point of a quadratic Bézier curve when prescribing a fixed arc length. It is a convex curve. Section 3 also studies the expression for the bending energy. Here, the region for the middle control point, when prescribing a particular bending energy, is not convex, thus the corresponding constraint problem may have multiple solutions.

Section 4 solves the design problem when introducing tangency constraints, to a circle or a line. It also gives performance results when implementing the computations on the GPU in Section 5. Because of the preceding locus analysis, the algorithms for solving these constraint problems are very simple. Section 6 discusses the circle transition problem for quadratic Bézier curves optimizing length and energy.

2 Definitions and Preliminaries

We consider quadratic Bézier curves $\mathbf{q}(t) = \sum_{i=0}^{2} \mathbf{b}_i B_i^2(t)$ where the $\mathbf{b}_i$ are control points and $B_i^n(t)$ are the familiar Bernstein-Bézier basis functions of degree n. We are interested in the *arc length* of those curves, given by the integral

$$L(\mathbf{q}) = \int_0^1 \sqrt{\mathbf{q}'(t) \cdot \mathbf{q}'(t)} dt \tag{1}$$

where $\mathbf{q}'(t)$ is the derivative of $\mathbf{q}(t)$ and $\cdot$ denotes the inner product. The integral has a closed form solution; see, e.g., [21]. Likewise, we consider those curves that have a given *bending energy*, given by

$$\mathcal{E}(\mathbf{q}) = \frac{1}{2} \int_{\mathbf{q}} \kappa(s)^2 ds \tag{2}$$

where $\kappa(s)$ is the curvature at s. We will express some relations in terms of a quantity Λ_α, defined as

$$\Lambda_\alpha = \alpha |\Delta \mathbf{b}_0|^2 + (1-\alpha)|\Delta \mathbf{b}_1|^2 - \frac{1}{4}|\Delta \mathbf{b}_2|^2$$

where $\Delta \mathbf{b}_i$ denotes the vector $\mathbf{b}_{i+1} - \mathbf{b}_i$, for $i = 0, 1$, and $\Delta \mathbf{b}_2 = \mathbf{b}_0 - \mathbf{b}_2$. Also, $|\cdot|$ denotes the length of a vector.

Throughout, we are interested in the locus of the middle control point $\mathbf{b}_1$. When considering tangency to a line, the *tangency locus* is a curve on which the middle control point must lie for the curve to realize the prescribed tangency, a line parallel to the tangent. For a circle, the *tangency locus* is more complicated and is analyzed in Section 4. For a fixed arc length and fixed end points $\mathbf{b}_0$ and $\mathbf{b}_2$, the possible positions of $\mathbf{b}_1$ comprise an *arc length locus*. Likewise, for fixed energy we have an *energy locus*. We will solve the problems stated in the introduction by intersecting these loci using a highly parallel GPU implementation.

3 Length and Energy of Quadratic Bézier Curves

We give analytic expressions for arc length and bending energy of quadratic Bézier curves. Arc length is stated in terms of the length of the sides and the area of the triangle $\triangle\mathbf{b}_0\mathbf{b}_1\mathbf{b}_2$. We also prove that the level sets of the arc length, for fixed curve end points, are convex. That is, fixing the end points $\mathbf{b}_0$ and $\mathbf{b}_2$, the locus of $\mathbf{b}_1$ for quadratic Bézier curves of fixed length is a convex curve. We then give a bending energy formula. Here, the level sets for given bending energy are no longer convex.

3.1 Arc Length

Let $\mathbf{q}(t)$, $t \in [0,1]$ be a quadratic Bézier curve with control points $\mathbf{b}_0$, $\mathbf{b}_1$ and $\mathbf{b}_2$. For such Bézier curves the arc length, defined by Equation (1), can be expressed as

$$\begin{aligned}\mathcal{L}(\mathbf{q}) = &\frac{\Lambda_{1/4}|\Delta\mathbf{b}_1| + \Lambda_{3/4}|\Delta\mathbf{b}_0|}{2\Lambda_{1/2}} \\ &+ \frac{|\Delta\mathbf{b}_0 \times \Delta\mathbf{b}_1|^2}{8(\Lambda_{1/2})^{3/2}}\Big\{\ln(\Lambda_{1/4} + |\Delta\mathbf{b}_1|\sqrt{\Lambda_{1/2}}) - \ln(-\Lambda_{3/4} + |\Delta\mathbf{b}_0|\sqrt{\Lambda_{1/2}})\Big\}.\end{aligned} \tag{3}$$

See also [7].

When both end points $\mathbf{b}_0$ and $\mathbf{b}_2$ are given, we can determine the orbits of the control point $\mathbf{b}_1 = [x_1, y_1]$ for which the Bézier curves have the same arc length. Figure 1 shows four orbits of $\mathbf{b}_1$s, for arc lengths 2.05, 2.5, 3, and 3.5, with $\mathbf{b}_0 = [-1, 0]$ and $\mathbf{b}_2 = [1, 0]$. We prove that the orbits are the boundary of convex sets.

LEMMA 3.1 *For fixed* $\mathbf{b}_0$ *and* $\mathbf{b}_2$*, the set* $S_L = \{\mathbf{b}_1 : \mathcal{L}(\mathbf{q}) \leq L\}$ *is convex.*

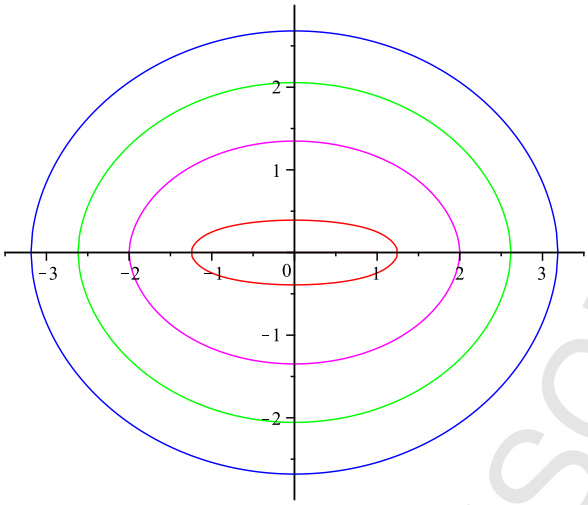

Fig. 1. Orbits of the middle control points $\mathbf{b}_1$ for curves with the same arc length 2.05(red), 2.5(magenta), 3(green), 3.5(blue), respectively, when $\mathbf{b}_0 = [-1, 0]$ and $\mathbf{b}_2 = [1, 0]$.

Proof. Let $[k_1, h_1], [k_2, h_2] \in S_L$ be two points in S_L. We will show that the convex combination $[k_3, h_3] = \lambda[k_1, h_1] + (1-\lambda)[k_2, h_2]$, with $\lambda \in (0, 1)$, is also in S_L.

For $j = 1, 2, 3$, let $\mathbf{q}^j(t)$ be the quadratic Bézier curve having the control points $\mathbf{b}_0, \mathbf{b}_1^j = [k_j, h_j], \mathbf{b}_2$, respectively, and let $\mathbf{b}_0^j = \mathbf{b}_0$ and $\mathbf{b}_2^j = \mathbf{b}_2$. Then

$$\mathbf{q}^3(t) = \sum_{i=0}^{2} B_i^2(t)\mathbf{b}_i^3 = \sum_{i=0}^{2} B_i^2(t)[\lambda\mathbf{b}_i^1 + (1-\lambda)\mathbf{b}_i^2] = \lambda\mathbf{q}^1(t) + (1-\lambda)\mathbf{q}^2(t)$$

For any partition $\{t_0 = 0, t_1, \cdots, t_{n-1}, t_n = 1\}$, by the triangle inequality

$$|\mathbf{q}^3(t_{k+1}) - \mathbf{q}^3(t_k)| \le \lambda|\mathbf{q}^1(t_{k+1}) - \mathbf{q}^1(t_k)| + (1-\lambda)|\mathbf{q}^2(t_{k+1}) - \mathbf{q}^2(t_k)|.$$

Thus

$$\mathcal{L}(\mathbf{q}^3) = \sup \sum_{k=1}^{n} |\mathbf{q}^3(t_{k+1}) - \mathbf{q}^3(t_k)| \le \lambda\mathcal{L}(\mathbf{q}^1) + (1-\lambda)\mathcal{L}(\mathbf{q}^2)$$

where the sup is for all partitions of the whole interval $[0, 1]$. Since $\mathcal{L}(\mathbf{q}^1)$ and $\mathcal{L}(\mathbf{q}^2)$ is less than or equal to L, so is $\mathcal{L}(\mathbf{q}^3)$. Thus the set $\{[k, h] : \mathbf{b}_1 = [k, h], \mathcal{L}(\mathbf{q}) \le L\}$ is convex. □

By the above lemma, it follows that the boundary $\{\mathbf{b}_1 : \mathcal{L}(\mathbf{q}) = L\}$ is a convex curve.

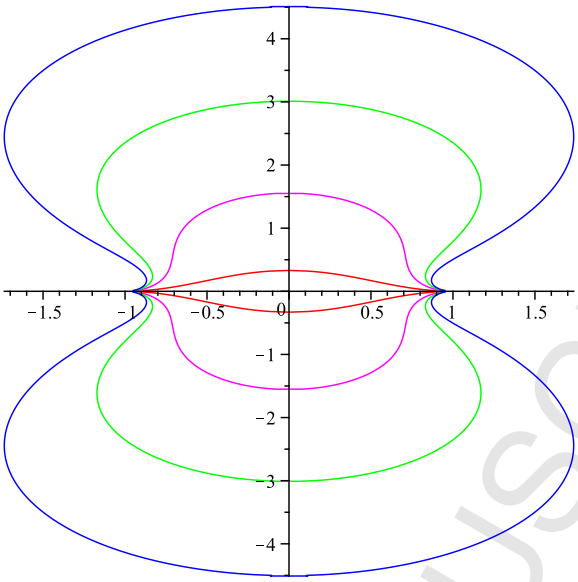

Fig. 2. Level curves of the energy function $\mathcal{E}(\mathbf{q}) = E$ of the quadratic Bézier curve $\mathbf{q}(t)$ with respect to the middle control point $\mathbf{b}_1$, where $E = 0.1$(red), 1(magenta), 2(green), or 3(blue), for fixed end points $\mathbf{b}_0 = [-1, 0]$ and $\mathbf{b}_2 = [1, 0]$.

3.2 Bending Energy

We consider now the bending energy of the Bézier curve $\mathbf{q}(t)$ defined by Equation (2). By algebra and using integral formulae, the bending energy can be expressed as

$$\mathcal{E}(\mathbf{q}) = \frac{2}{3|\Delta\mathbf{b}_0 \times \Delta\mathbf{b}_1|^2}\,(A + B) \tag{4}$$

where

$$A = \frac{\Lambda_{1/4}(3\Lambda_{1/2}|\Delta\mathbf{b}_1|^2 - \Lambda_{1/4}^2)}{|\Delta\mathbf{b}_1|^3} \quad \text{and} \quad B = \frac{\Lambda_{3/4}(3\Lambda_{1/2}|\Delta\mathbf{b}_0|^2 - \Lambda_{3/4}^2)}{|\Delta\mathbf{b}_0|^3}.$$

For fixed $\mathbf{b}_0$ and $\mathbf{b}_2$, we can determine the locus of the control point $\mathbf{b}_1 = [x_1, y_1]$ for which the Bézier curves have the same energy. Figure 2 shows four contours, for energy 0.1, 1, 2, and 3, when $\mathbf{b}_0 = [-1, 0]$ and $\mathbf{b}_2 = [1, 0]$.

We explore the level curves near the singularities. By symmetry, it suffices to explore the curves near the control point $\mathbf{b}_0$. In the following, we assume that $\mathbf{b}_0 = [-1, 0]$ and $\mathbf{b}_2 = [1, 0]$. Let r be the distance $|\Delta\mathbf{b}_0|$ and let θ be the angle between the x-axis and the vector $\Delta\mathbf{b}_0$, in the positive orientation. Observing

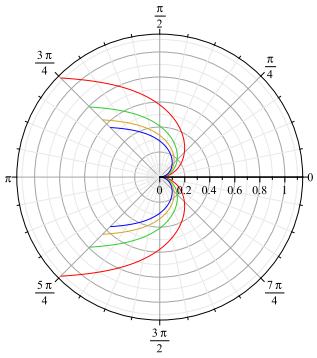

Fig. 3. Energy level curves near the singularity at $\mathbf{b}_0$ for E=1(red) to E=4(blue).

that $|\Delta\mathbf{b}_2| = 2$, we estimate $\mathcal{E}(\mathbf{q})$ for $r \ll 1$ (cf. Equation (4)). We have

$$\begin{aligned}
\frac{2}{3|\Delta\mathbf{b}_0 \times \Delta\mathbf{b}_1|^2} &= \frac{1}{6r^2\sin^2\theta} \\
\Lambda_{1/4} &\approx 2 - 3r\cos\theta \\
\Lambda_{1/2} &\approx 1 - 2r\cos\theta \\
\Lambda_{3/4} &\approx -r\cos\theta \\
A &\approx 2 - 6r\cos\theta \\
B &\approx \cos^3\theta - 3\cos\theta
\end{aligned}$$

so that, neglecting the $O(r)$ term of the approximation of A, we obtain for sufficiently small r:

$$\mathcal{E}(\mathbf{q}) \approx \frac{(\cos\theta + 2)\tan^2(\theta/2)}{6r^2} \tag{5}$$

The estimate implies that the level curves of equal energy reach the singularities at $\mathbf{b}_0$ and $\mathbf{b}_2$ tangent to the x-axis. Moreover, fixing $\theta < 2\pi$ and for small r, the energy $\mathcal{E}(\mathbf{q})$ is proportional to $1/r^2$. Figure 3 shows several level curves near the singularity at $\mathbf{b}_0$. As the energy threshold is increased, the level curves curl more tightly near the singularity. It follows that the curves $\mathcal{E}(\mathbf{q}) = E$ are properly nested.

4 Tangency Locus

We fix the start and end points of the quadratic Bézier curve and construct the locus of the control point $\mathbf{b}_1$ of all curves that are tangent to a given geometric element T. This tangency locus is simple when T is a line, but it is considerably more complex when T is a circle.

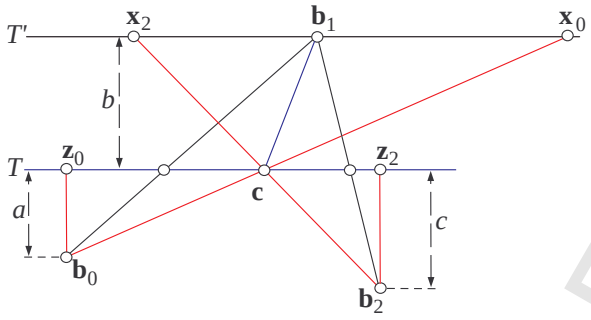

Fig. 4. Quadratic Bézier control points and tangency to line T.

4.1 Tangency to a Line

The tangency locus to a given line is particularly simple:

PROPOSITION 4.1 *Given a line T and two points $\mathbf{b}_0$ and $\mathbf{b}_2$ on the same side of T, let $\mathbf{q}(t)$ be a quadratic Bézier curve with control points $\mathbf{b}_k$, $k = 0, 1, 2$. Then the following holds (Figure 4).*

(a) *$\mathbf{q}(t)$ is tangent to T iff $\mathbf{b}_1$ is on the line T' parallel to T at a distance that is the geometric mean of the distances of $\mathbf{b}_0$ and $\mathbf{b}_2$ to T, and on the opposite side of $\mathbf{b}_0$ and $\mathbf{b}_2$. That is, $b^2 = ac$.*

(b) *With $\mathbf{c}$ the point of tangency on T, $\mathbf{b}_1$ is the midpoint of the intersections $\mathbf{x}_0$ and $\mathbf{x}_2$ of T' with the lines through $\mathbf{c}$ and $\mathbf{b}_0$ and $\mathbf{b}_2$, respectively.*

(c) *Let $\mathbf{z}_0$ and $\mathbf{z}_2$ be the orthogonal projections of $\mathbf{b}_0$ and $\mathbf{b}_2$ onto T. If the normal N through $\mathbf{c}$ contains the point $\mathbf{b}_1$, then N and T bisect the angles between the lines $\overline{\mathbf{b}_0\mathbf{c}}$ and $\overline{\mathbf{b}_2\mathbf{c}}$. Moreover, $\mathbf{c}$ divides the line segment $\overline{\mathbf{z}_0\mathbf{z}_2}$ in the ratio $a : c$.*

Proof. Let $\mathbf{y}_i$, $i = 0, 2$, be the intersection point of the lines T and $\overline{\mathbf{b}_1\mathbf{b}_i}$. By the de Casteljau algorithm, the line T is tangent to the Bézier curve iff $|\mathbf{b}_0 - \mathbf{y}_0| : |\mathbf{y}_0 - \mathbf{b}_1| = |\mathbf{b}_1 - \mathbf{y}_2| : |\mathbf{y}_2 - \mathbf{b}_2|$. With a, b and c the distances of the control points from T as shown in Figure 4, we have $|\mathbf{b}_0 - \mathbf{y}_0| : a = |\mathbf{y}_0 - \mathbf{b}_1| : b$ and $|\mathbf{b}_1 - \mathbf{y}_2| : b = |\mathbf{y}_2 - \mathbf{b}_2| : c$, and therefore $b^2 = ac$. Part (a) follows.

For Part (b), if $\mathbf{b}_1$ be the midpoint of $\mathbf{x}_0$ and $\mathbf{x}_2$, then

$$\frac{|\mathbf{y}_0 - \mathbf{c}|}{|\mathbf{b}_1 - \mathbf{x}_0|} = \frac{a}{a+b}, \qquad \frac{|\mathbf{x}_2 - \mathbf{b}_1|}{|\mathbf{c} - \mathbf{y}_2|} = \frac{b+c}{c}.$$

Since $ac = b^2$, the ratio $|\mathbf{y}_0 - \mathbf{c}| : |\mathbf{c} - \mathbf{y}_2|$ is equal to $a : b$, thus $\mathbf{c}$ is on $\mathbf{q}(t)$ with tangent T. The converse is argued analogously.

If the normal N through C contains $\mathbf{b}_1$, then the triangle $\triangle \mathbf{x}_0\mathbf{x}_2\mathbf{c}$ is isosceles, so T and N bisect the angles. Therefore, the triangles $\triangle \mathbf{b}_0\mathbf{z}_0\mathbf{c}$ and $\triangle \mathbf{b}_2\mathbf{z}_2\mathbf{c}$ are similar. This establishes Part (c). □

Given $\mathbf{b}_0, \mathbf{b}_2, \mathbf{c}$ and T, the missing control point $\mathbf{b}_1$ can be constructed using Part (b) of Proposition 4.1. If the control point is to lie on the normal through $\mathbf{c}$, then $\mathbf{c}$ can be found using Part (c).

4.2 Tangency to a Circle

Let a circle be given by $[x(\theta), y(\theta)] = [O_x + r\cos\theta, O_y + r\sin\theta]$, where $\mathbf{O} = [O_x, O_y]$ is the center and r is the radius of the circle, and $\mathbf{b}_0 = [x_0, y_0]$ and $\mathbf{b}_2 = [x_2, y_2]$ are the end points of the quadratic Bézier curve; Figure 5(a).

Let θ_j, $j = 1, \cdots, 4$ be the signed angles of the four tangent points on the circle of the lines(skyblue and orange) passing $\mathbf{b}_0$ and $\mathbf{b}_2$, as shown in Figure 5(a). By Proposition 4.1, the quadratic Bézier curve is tangent to the circle at the point $\mathbf{c}(\theta) = [x(\theta), y(\theta)]$ if and only if the middle control point $\mathbf{b}_1(\theta) = [x_1(\theta), y_1(\theta)]$ satisfies

$$\begin{aligned}&[x_1(\theta), y_1(\theta)] = \\ &\quad [x(\theta), y(\theta)] + \tfrac{1}{2}\left(\sqrt{\tfrac{d_2}{d_0}}[x(\theta) - x_0, y(\theta) - y_0] + \sqrt{\tfrac{d_0}{d_2}}[x(\theta) - x_2, y(\theta) - y_2]\right)\end{aligned} \tag{6}$$

$\theta_1 < \theta < \theta_2$ or $\theta_3 < \theta < \theta_4$, where d_i is the distance from $\mathbf{b}_i$ to the common tangent(green line) of circle and Bézier curve,

$$d_i = \frac{1}{r}|(x - x_i)(x - O_x) + (y - y_i)(y - O_y)| = \frac{|(\mathbf{c} - \mathbf{b}_i)\cdot(\mathbf{c} - \mathbf{O})|}{r}.$$

Let $\sigma = (\mathbf{c} - \mathbf{b}_0)\cdot(\mathbf{c} - \mathbf{O})/|(\mathbf{c} - \mathbf{b}_0)\cdot(\mathbf{c} - \mathbf{O})|$. It is obvious that $\sigma = (\mathbf{c} - \mathbf{b}_2)\cdot(\mathbf{c} - \mathbf{O})/|(\mathbf{c} - \mathbf{b}_2)\cdot(\mathbf{c} - \mathbf{O})|$, since the two points $\mathbf{b}_0$ and $\mathbf{b}_2$ are on the same side of the common tangent. If $\mathbf{b}_0$ and $\mathbf{O}$ lie on the same side of the common tangent, then $\sigma = 1$ and if they are on the opposite side, then $\sigma = -1$. Thus we obtain

$$d_i = \frac{\sigma}{r}\{(\mathbf{c} - \mathbf{b}_i)\cdot(\mathbf{c} - \mathbf{O})\}. \tag{7}$$

PROPOSITION 4.2 *The tangent of the tangency locus at $[x_1(\theta), y_1(\theta)]$ is parallel to the tangent of the circle at $[x(\theta), y(\theta)]$, for each $\theta \in (\theta_0, \theta_1) \cup (\theta_3, \theta_4)$. Furthermore they have the same tangent direction if the line segment $\overline{\mathbf{b}_0\mathbf{b}_2}$ and the center $\mathbf{O}$ lie on opposite sides of the common tangent of circle and Bézier curve.*

Proof. The derivative of $[x_1(\theta), y_1(\theta)]$ in Equation (6) is

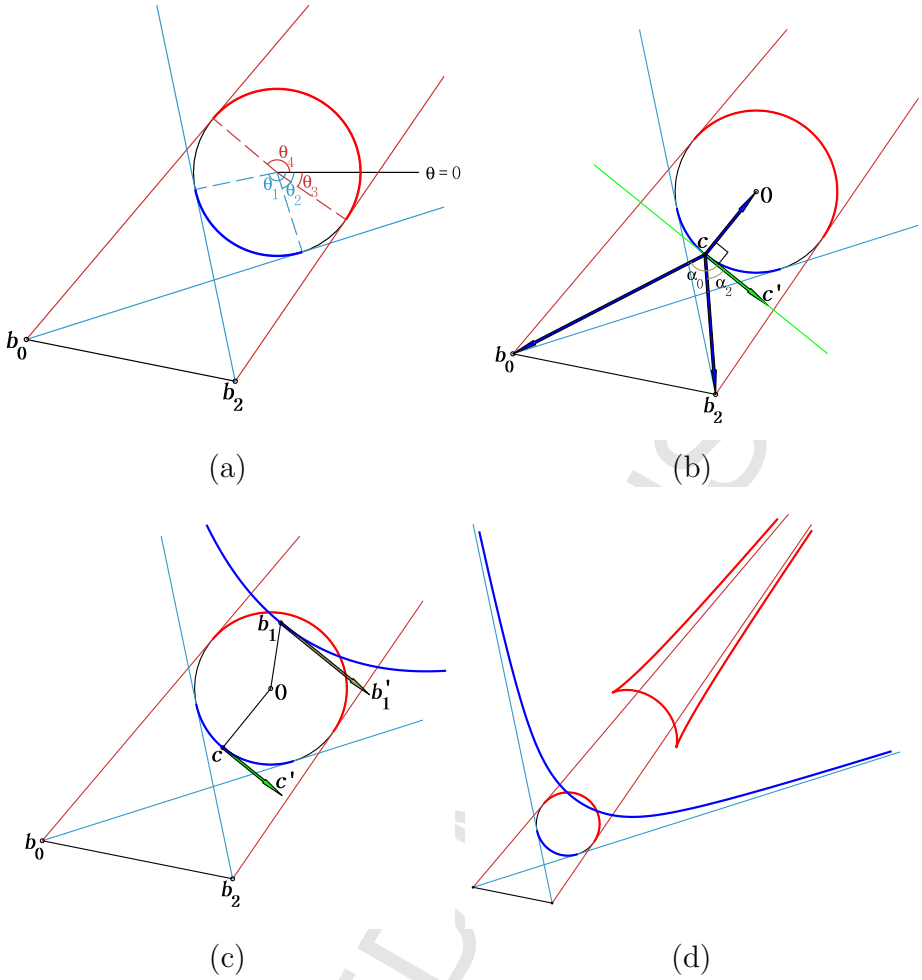

Fig. 5. (a) The quadratic Bézier curve with end points $\mathbf{b}_0$ and $\mathbf{b}_2$ has the contact point $\mathbf{c}(\theta)$ on the circle, $\theta_1 < \theta < \theta_2$ (closer arc, blue) and $\theta_3 < \theta < \theta_4$ (farther arc, red). (b) On the closer branch, the center $\mathbf{O}$ and the line segment $\overline{\mathbf{b}_0\mathbf{b}_2}$ are on opposite sides of the common tangent(green line). (c) $\mathbf{c}'(\theta)$ and $\mathbf{b}_1'(\theta)$ are parallel and have the same direction for the closer branch of the tangency locus(blue curve). (d) The tangency locus of $\mathbf{b}_1$ consists of two branches, closer branch(blue curve) and farther branch(red curve).

$$[x_1'(\theta), y_1'(\theta)] = [x'(\theta), y'(\theta)] \left(1 + \frac{1}{2}\left(\sqrt{\frac{d_2}{d_0}} + \sqrt{\frac{d_0}{d_2}}\right)\right) + \frac{1}{2}\frac{d_0 d_2' - d_0' d_2}{d_0^{3/2} d_2^{3/2}} \{d_2(\mathbf{c}(\theta) - \mathbf{b}_0) - d_0(\mathbf{c}(\theta) - \mathbf{b}_2)\}. \tag{8}$$

From Equation (7) we get

$$d_2(\mathbf{c}(\theta) - \mathbf{b}_0) - d_0(\mathbf{c}(\theta) - \mathbf{b}_2) = \frac{\sigma}{r}((\mathbf{c} - \mathbf{b}_0) \times (\mathbf{c} - \mathbf{b}_2))[y - O_y, -(x - O_x)] \tag{9}$$

Since the vector $[y - O_y, -(x - O_x)]$ is parallel to $[x'(\theta), y'(\theta)]$, we have

$$[x_1'(\theta), y_1'(\theta)] \parallel [x'(\theta), y'(\theta)].$$

If the line segment $\overline{\mathbf{b}_0\mathbf{b}_2}$ and the center $\mathbf{O}$ lie on opposite sides of the common tangent, then $\sigma = -1$ and Equation (9) yields

$$d_2(\mathbf{c}(\theta) - \mathbf{b}_0) - d_0(\mathbf{c}(\theta) - \mathbf{b}_2) = \frac{1}{r}\left((\mathbf{c} - \mathbf{b}_0) \times (\mathbf{c} - \mathbf{b}_2)\right)\mathbf{c}'(\theta), \qquad (10)$$

which is the same direction as $[x'(\theta), y'(\theta)]$. Since $\mathbf{c}'(\theta) \cdot (\mathbf{c}(\theta) - \mathbf{O}) = 0$, we have $d_i'(\theta) = \frac{-1}{r}\,\mathbf{c}'(\theta) \cdot (\mathbf{c} - \mathbf{b}_i)$ for $i = 0, 2$, and

$$d_0d_2' - d_0'd_2 = \frac{1}{r^2}((\mathbf{c}-\mathbf{b}_0)\cdot(\mathbf{c}-\mathbf{O}))\,(\mathbf{c}'\cdot(\mathbf{c}-\mathbf{b}_2)) - \frac{1}{r^2}((\mathbf{c}-\mathbf{b}_2)\cdot(\mathbf{c}-\mathbf{O}))\,(\mathbf{c}'\cdot(\mathbf{c}-\mathbf{b}_0)).$$

Let α_i be the angle between the two vectors $\mathbf{c}'$ and $\mathbf{b}_i - \mathbf{c}$, for $i = 0, 2$, as shown in Figure 5(b). Then

$$d_0d_2' - d_0'd_2 = \frac{1}{r^2}|\mathbf{c}-\mathbf{b}_0||\mathbf{c}-\mathbf{O}||\mathbf{c}'||\mathbf{c}-\mathbf{b}_2|(-\cos(\frac{\pi}{2}+\alpha_0)\cos\alpha_2 + \cos(\frac{\pi}{2}+\alpha_2)\cos\alpha).$$

Since $0 < \alpha_2 < \alpha_0 < \pi$, we have

$$d_0d_2' - d_0'd_2 = \frac{1}{r^2}|\mathbf{c} - \mathbf{b}_0||\mathbf{c} - \mathbf{O}||\mathbf{c}'||\mathbf{c} - \mathbf{b}_2| \cdot \sin(\alpha_0 - \alpha_2) > 0. \qquad (11)$$

By Equations (8)-(11), $[x_1(\theta), y_1(\theta)]$ has the same tangent direction to $[x(\theta), y(\theta)]$. □

Remark 4.3 *(a) As shown in Figure 5, the contact points* $\mathbf{c}$ *of the circle and the quadratic Bézier curve lie on two arcs, a closer arc(blue curve) and a farther arc(red curve), from the line segment* $\overline{\mathbf{b}_0\mathbf{b}_2}$*. Likewise, the middle control points* $\mathbf{b}_1$ *form two branches of the tangency locus.*

(b) By Proposition 4.2, the Gauss maps of the tangency locus and of the contact point arcs are equal by components:[1]

$$\mathcal{N}(\{\mathbf{c}(\theta) : \theta_1 < \theta < \theta_2\}) = \mathcal{N}(\{\mathbf{b}_1(\theta) : \theta_1 < \theta < \theta_2\})$$
$$\mathcal{N}(\{\mathbf{c}(\theta) : \theta_3 < \theta < \theta_4\}) = \mathcal{N}(\{\mathbf{b}_1(\theta) : \theta_3 < \theta < \theta_4\}).$$

Even if the curve $[x(\theta), y(\theta)]$ *is not a circle, the above two equations are true whenever the curve is* C^1*-continuous.*

(c) By Equations (6) and (7), the tangency locus of $\mathbf{b}_1$ *has the four assymptotic lines(skyblue and orange).*

[1] For more about the Gauss map, see [18,25,26].

COROLLARY 4.4 *The closer branch of tangency locus of* $\mathbf{b}_1$ *is nonsingular.*

Proof. By Proposition 4.2, $\mathbf{b}_1'(\theta)$ is parallel and has the same direction to $\mathbf{c}'(\theta)$, i.e., $\mathbf{b}_1'(\theta) = k \cdot \mathbf{c}'(\theta)$ for some positive real number $k > 0$. Since $\mathbf{c}'(\theta)$ is a nonzero vector for all $\theta \in (\theta_1, \theta_2)$, so is $\mathbf{b}_1'(\theta)$, and the closer branch(blue curve) of tangency locus of $\mathbf{b}_1$ is nonsingular, as illustrated in Figure 5. □

PROPOSITION 4.5 *If any point on the line segment* $\overline{\mathbf{b}_0\mathbf{b}_2}$ *is neither inside nor on the circle* C*, then the minimum length quadratic Bézier curve has the middle control point* $\mathbf{b}_1$ *on the closer branch* $\{\mathbf{b}_1(\theta) : \theta_1 < \theta < \theta_2\}$*, not on the farther branch* $\{\mathbf{b}_1(\theta) : \theta_3 < \theta < \theta_4\}$*.*

Proof. If any point on the line segment $\overline{\mathbf{b}_0\mathbf{b}_2}$ is neither inside nor on the circle C, then the closer branch $\{\mathbf{b}_1(\theta) : \theta_1 < \theta < \theta_2\}$ is not empty. By the definition of $\mathbf{b}_1$ in Equation (6), the closer branch and the farther branch each are connected sets in the plane. By Remark 4.3(c), the closer branch has two asymptotic lines, so it separates the plane into two regions. One region contains the line segment $\overline{\mathbf{b}_0\mathbf{b}_2}$, and the other region contains the far branch.

Assume that the minimum length is attained at $\mathbf{b}_1^f$ on the far branch. Let $\mathbf{m}$ be the midpoint of $\mathbf{b}_0$ and $\mathbf{b}_2$. The line segment $\overline{\mathbf{b}_1^f\mathbf{m}}$ intersects the closer branch, say, $\mathbf{b}_1^c$. By convexity, Lemma 3.1, there exists some $\lambda \in (0, 1)$ such that

$$\mathcal{L}(\mathbf{b}_1^c) = \lambda\mathcal{L}(\mathbf{b}_1^f) + (1-\lambda)\mathcal{L}(\mathbf{m}) < \mathcal{L}(\mathbf{b}_1^f)$$

which is a contradiction. Hence the minimum length is obtained on the closer branch $\{\mathbf{b}_1(\theta) : \theta_1 < \theta < \theta_2\}$ and not on the far branch $\{\mathbf{b}_1(\theta) : \theta_3 < \theta < \theta_4\}$. □

We have a number of special cases, when the line segment $\overline{\mathbf{b}_0\mathbf{b}_2}$ intersects the circle C or lies inside C. These can be classified into six different cases, as shown in Figure 6.

PROPOSITION 4.6 *The tangency locus of* $\mathbf{b}_1$ *has the following properties.*

(a) *The tangency locus of* $\mathbf{b}_1$ *is bounded if and only if both end-points* $\mathbf{b}_0$ *and* $\mathbf{b}_2$ *lie inside the circle.*
(b) *If one end-point is on* C *and the other is inside* C*, then the tangency locus of* $\mathbf{b}_1$ *consists of one straight line and a bounded curve.*
(c) *If two control points* $\mathbf{b}_0$ *and* $\mathbf{b}_2$ *lie on the circle, then the tangency locus consists of two straight lines and two circular arcs that are centered at the points* $\mathbf{O} \pm \frac{r}{|\mathbf{m}-\mathbf{O}|}(\mathbf{m}-\mathbf{O})$*, on the circle perimeter, with the radius* $r \mp |\mathbf{m}-\mathbf{O}|$*.*

Proof. (a) Assume that at least one of the two points $\mathbf{b}_0$ and $\mathbf{b}_1$ lies outside the circle C, say $\mathbf{b}_0$. Let $\mathbf{c}(\theta_1)$ be the tangent point from $\mathbf{b}_0$ to the circle, and

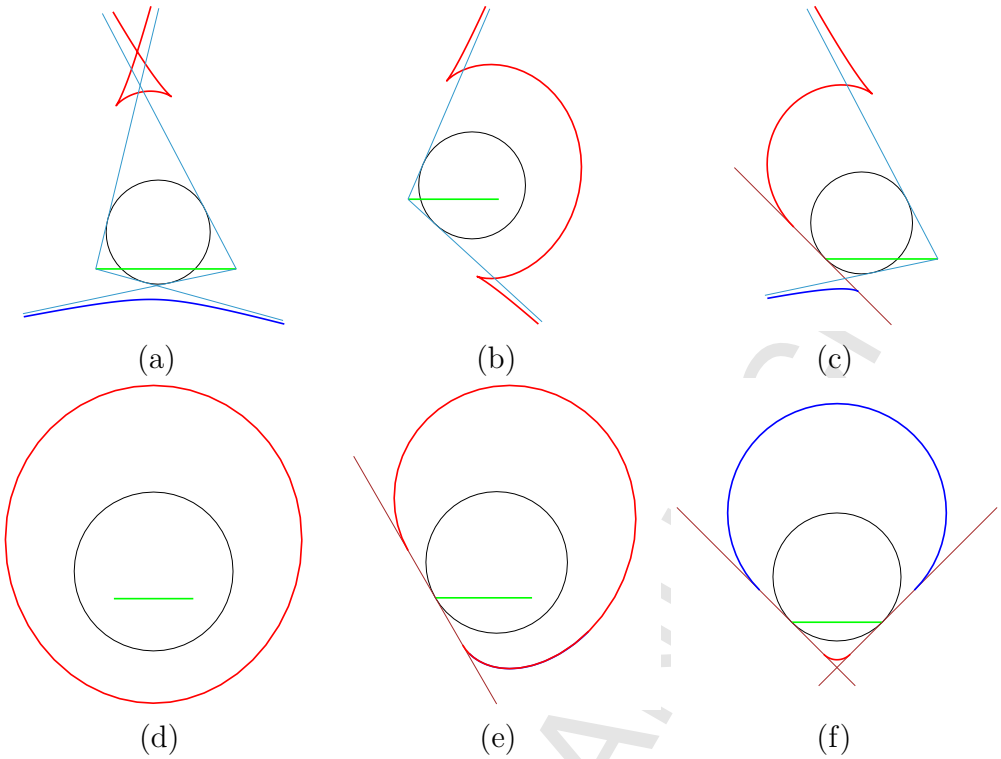

Fig. 6. Tangency locus for a circle. There are six special cases. (a) both end points $\mathbf{b}_0$ and $\mathbf{b}_2$ lie outside the (gray) circle C, (b) one end point is outside and the other is inside, (c) one is outside and the other lies on C, (d) both are inside C, (e) one is on C and the other is inside, or (f) both lie on the circle C. The green line connects $\mathbf{b}_0$ and $\mathbf{b}_2$. In cases (c), (e) and (f) the tangency locus includes, as a component, the circle tangent of an end point on the perimeter.

$\{\mathbf{b}_1(\theta) : \theta \in (\theta_1, \theta_2)\}$ a part of the tangency locus of $\mathbf{b}_1$. As θ approaches θ_1 from the right, $d_0(\theta)$ converges to zero, and $d_2(\theta)$ and $\mathbf{c}(\theta) - \mathbf{b}_0$ converge to nonzero limits, so $|\mathbf{b}_1(\theta)|$ diverges to ∞ by Equation (6). Thus the tangency locus is unbounded and the line $\overline{\mathbf{b}_0\mathbf{c}(\theta_1)}$ is an asymptote, as shown in Figures 5 and 6(a)-(c).

Let at least one of two end-points lie on the circle C, say $\mathbf{b}_0$. Let ℓ_0 be the circle tangent at $\mathbf{b}_0$. If $\mathbf{b}_1$ lies on the line ℓ_0, then the quadratic Bézier curve $\mathbf{q}$ having the control points $\mathbf{b}_i$, $i = 0, 1, 2$ is tangent to the circle C at $\mathbf{q}(0) = \mathbf{b}_0$. Thus the straight line ℓ_0 is a part of the tangency locus of $\mathbf{b}_1$ and so the tangency locus is unbounded, as shown in Figure 6(c), (e) and (f).

Let both end-points be inside C. Then $\{\mathbf{b}_1(\theta) : \theta \in [0, 2\pi]\}$ is the tangency locus of $\mathbf{b}_1$. Since for $i = 0, 2$, $d_i(\theta)$ is non-zero continuous and $\mathbf{c}(\theta) - \mathbf{b}_i$ is continuous, so is $\mathbf{b}_1(\theta)$ by Equation (6). Thus the tangency locus is a compact set in the plane, which means that it is closed and bounded[24], as shown in Figure 6(d).

(b) Let one of $\mathbf{b}_1$ or $\mathbf{b}_2$ lie on C and the other inside C. Without loss of generality, we may assume that $\mathbf{b}_0$ is on C and $\mathbf{b}_2$ inside C. Let ℓ_0 be the tangent line of the circle at the point $\mathbf{b}_0$. For some $\theta_0 \in [0, 2\pi)$, $\mathbf{b}_0 = \mathbf{c}(\theta_0)$, and the tangency locus of $\mathbf{b}_1$ consists of $\{\mathbf{b}_1(\theta) : \theta \in (\theta_0, \theta_0 + 2\pi)\}$ and ℓ_0. Since $d_0(\theta) = |\mathbf{c} - \mathbf{b}_0|^2/2r$, both limits

$$\lim_{\theta \to \theta_0^{\pm}} \sqrt{\frac{d_2(\theta)}{d_0(\theta)}}(\mathbf{c} - \mathbf{b}_0) = \sqrt{2r d_2(\theta_0)} \cdot (\pm T_0)$$

exist, where T_0 is the unit tangent vector of $\mathbf{c}(\theta)$ at $\theta = \theta_0$. Thus $\mathbf{b}_1(\theta)$ can be extended continuously at both end points $\theta = \theta_0$ and $\theta_0 + 2\pi$, which is the compactification[24]. Hence the extended set $\{\mathbf{b}_1(\theta) : \theta \in [\theta_0, \theta_0 + 2\pi]\}$ is compact, and so the tangency locus consists ℓ_0 and a bounded curve, as shown in Figure 6(e).

(c) Let both end points $\mathbf{b}_0$ and $\mathbf{b}_2$ lie on the circle. For $i = 0, 2$, let ℓ_i be the tangent line of the circle at the point $\mathbf{b}_i$. For some θ_0 and θ_2 with $\theta_0 < \theta_2 < \theta_0 + 2\pi$, $\mathbf{c}(\theta_0) = \mathbf{b}_0$ and $\mathbf{c}(\theta_2) = \mathbf{b}_2$. The tangency locus of $\mathbf{b}_1$ consists ℓ_0, ℓ_2 and $\{\mathbf{b}_1(\theta) : \theta \in (\theta_0, \theta_2), (\theta_2, \theta_0 + 2\pi)\}$. For $\theta \in (\theta_0, \theta_2)$, $d_i(\theta) = |\mathbf{c} - \mathbf{b}_i|^2/2r$, $i = 0, 2$ and

$$|\mathbf{c} - \mathbf{b}_0| = 2r \sin\frac{\theta - \theta_0}{2}, \qquad |\mathbf{c} - \mathbf{b}_2| = 2r \sin\frac{\theta_2 - \theta}{2}.$$

Thus by Equation (6) and trigonometry, we have

$$\mathbf{b}_1(\theta) = r(1 - \cos\frac{\theta_2 - \theta_0}{2})[\cos\theta, \sin\theta] + [O_x + r\cos\frac{\theta_0 + \theta_2}{2}, O_y + r\sin\frac{\theta_0 + \theta_2}{2}].$$

Analogously, for $\theta \in (\theta_2, \theta_0 + 2\pi)$,

$$\mathbf{b}_1(\theta) = r(1 + \cos\frac{\theta_2 - \theta_0}{2})[\cos\theta, \sin\theta] + [O_x - r\cos\frac{\theta_0 + \theta_2}{2}, O_y - r\sin\frac{\theta_0 + \theta_2}{2}].$$

Hence the tangency locus consists of two strait lines and two circular arcs centered at $\mathbf{O} \pm \frac{r}{|\mathbf{m}-\mathbf{O}|}(\mathbf{m} - \mathbf{O})$ with the radius $r \mp |\mathbf{m} - \mathbf{O}|$, as shown in Figure 6(f). □

5 Implementation and Results

We have implemented the construction of quadratic Bézier curves subject to tangency and length or energy minimization constraints. The basic algorithm amounts to sampling candidate contact points, along the stipulated tangent or tangency circle, and evaluate the resulting arc length or bending energy. This very fast computation uncovers local minima that can be refined iteratively or

by oversampling subregions. The sampling can be implemented in the GPU. However, because of the simplicity of the task and the simplicity of the domain, we elected to keep this computation in the CPU. Our implementation includes the option of computing the $\mathbf{b}_1$ tangency locus, analyzed before, as well as the $\mathbf{b}_1$ locus of the energy and arc length level sets. The latter curves are computed in the GPU using continuation.

By Propositions 4.1, the $\mathbf{b}_1$ tangency locus is a parallel to the tangent line. By Lemma 3.1, moreover, the minimum-length solution is unique. We noticed empirically that the minimum length solution is achieved near a tangency at which the curve normal contains the $\mathbf{b}_1$ control point. This is a suitable starting point for iteratively determining the solution. For tangency to a circle we cannot expect a unique minimum solution. For instance, when the end points lie symmetrically with respect to the circle center there will be two global arc length minima.

We measured the program performance on a desktop PC outfitted with a desktop PC running Windows Vista (32bit) with the following configuration: Intel Xeon X5460 CPU at 3.16GHz, 4GB main memory, and an nVidia GeForce GTX 285 graphics card driving a display with 2560x1600 pixels. The program was run in release mode alongside other applications. Performance is impacted by whether level set loci are computed, and so we measured performance with and without this computation. All performance numbers are in frames per second (fps) and are obtained by moving the start or endpoint with the mouse. Thus, 500 fps means that the computation to update the display takes only 2 msec.

	no level sets	level sets
Minimum length line tangent	2000	340
Minimum length circle tangent	1400	300
Minimum energy line tangent	2000	300
Minimum energy circle tangent	1290	275

Figure 7 shows a representative screen shot.

6 The Circle Transition Problem

We now consider the *Circle Transition Problem* that asks to connect tangentially two given circles with a Bézier curve. In this section, we deal with the following variant of the circle transition problem:

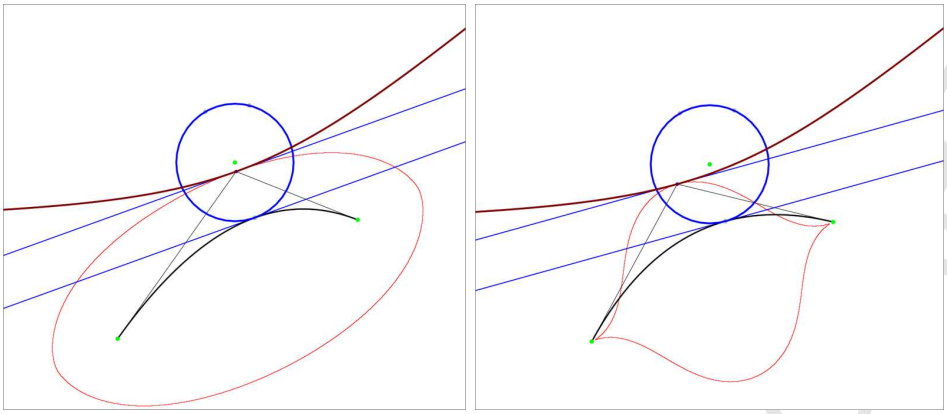

Fig. 7. *Left:* minimum length quadratic Bézier curve (black) tangent to a circle; length locus red, tangency locus brown. *Right:* minimum energy quadratic Bézier curve (black) tangent to a circle; energy locus red, tangency locus brown.

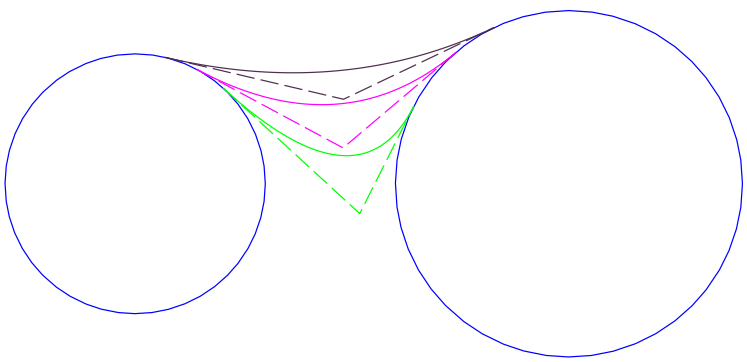

Fig. 8. The quadratic circle-transitions which are tangent to two given circles(blue) and minimize $\mu\mathcal{L}(\mathbf{q}) + (1-\mu)\mathcal{E}(\mathbf{q})$ for $\mu = 1$(green), $\mu = 1/10$(magenta), and $\mu = 1/30$(khaki), and their control polygons(dash-lines).

For real numbers $0 < \mu < 1$, find a parabolic arc tangent to two circles that minimizes the convex combination of length and bending energy as

$$\min\left(\mu\mathcal{L}(\mathbf{q}) + (1-\mu)\mathcal{E}(\mathbf{q})\right) \tag{12}$$

Using the formulae (3) and (4), we obtain the parabolic arc which is a circle transition of two given circles and satisfies Equation (12). Figure 8 shows examples for $\mu = 1, 1/10$ and $1/30$. The offset curves of the parabolic arcs and circles can then be obtained directly as rational Bézier curves. Figure 9 shows the offset curves of the circle transitions shown in Figure 8.

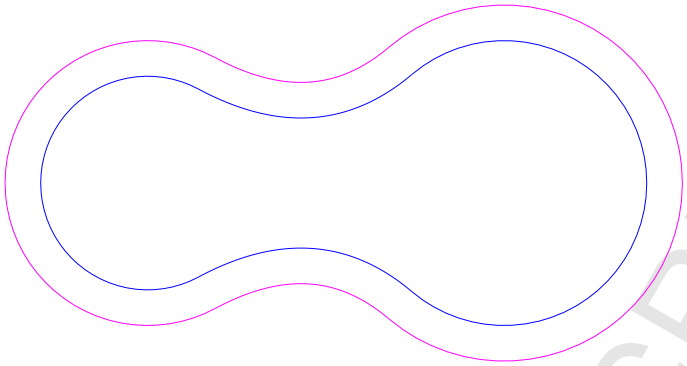

Fig. 9. Offset curve(magenta) of two circles and quadratic circle-transition(blue) for $\mu = 1/10$.

7 Acknowledgement

This work was supported by Basic Science Research Program through the National Research Foundation of Korea(NRF) funded by the Ministry of Education, Science and Technology (2011-0010147); by grants CPATH 0722210 and CPATH 0938999 of the US National Science Foundation; and by a gift from the Intel Corporation. The authors are grateful to the editor and two anonymous referees for their valuable comments and constructive suggestions.

References

[1] Y. J. Ahn and C. M. Hoffmann. Constraint-based LN-curves. In *Proc. ACM Symp. Appl. Computing*, Sierre, Switzerland, 2010.

[2] Y. J. Ahn and C. M. Hoffmann. Approximate convolution with pairs of cubic Bézier LN curves. *Comp. Aided Geom. Desi.*, 28:357–367, 2011.

[3] Y. J. Ahn, C. M. Hoffmann, and Y. S. Kim. Curvature-continuous offset approximation based on circle approximation using quadratic Bézier biarcs. *Comp. Aided Desi.*, 43:1011–1017, 2011.

[4] C. L. Bajaj, J. Chen, R. J. Holt, and A. N. Netravali. Energy formulations of A-splines. *Computer Aided Geometric Design*, 16:39–59, 1999.

[5] F. Bao, Q. Sun, J. Pan, and Q. Duan. A blending interpolator with value control and minimal strain energy. *Computers and Graphics*, 34:119–124, 2010.

[6] B. Bettig and C. Hoffmann. Geometric constraint solving in parametric Computer-Aided Design. *J. Comput. Inf. Sci. Eng.*, 11:021001, 2011.

[7] E. Boebert. Computing the arc length of cubic Bézier curves, 1993. http://steve.hollasch.net/cgindex/curves/cbezarclen.html, accessed 2010.

[8] G. Brunnett and J. Kiefer. Interpolation with minimal-energy splines. *CAD*, 26:137–144, 1994.

[9] R. Farouki. The elastic bending energy of Pythagorean-hodograph curves. *CAGD*, 13:227–241, 1996.

[10] R. T. Farouki and T. W. Sederberg. Analysis of the offset to a parabola. *Comp. Aided Geom. Desi.*, 12(6):639–645, 1995.

[11] G. E. Fasshauer and L. L. Schumaker. Minimal energy surfaces using parametric splines. *Computer Aided Geometric Design*, 13:45–79, 1996.

[12] M. S. Floater. Arc length estimation and the convergence of polynomial curve interpolation. *Journal BIT Numerical Mathematics*, 45:679–694, 2005.

[13] J. Gravesen. Adaptive subdivision and the length and energy of Bézier curves. *Computational Geometry*, 8:13–31, 1997.

[14] Z. Habib and M. Sakai. G^2 PH quintic spiral transition curves and their applications. *Scientiae Mathematicae Japonicae*, 61:207–218, 2005.

[15] Z. Habib and M. Sakai. Spiral transition curves and their applications. *Scientiae Mathematicae Japonicae*, 61:195–206, 2005.

[16] Z. Habib and M. Sakai. G^2 cubic transition between two circles with shape control. *Comp. Aided Desi.*, 39:125–132, 2007.

[17] Z. Habib and M. Sakai. On PH quintic spirals joining two circles with one circle inside the other. *J. Comp. Appl. Math.*, 223:133–144, 2009.

[18] S. Hur and T. Kim. Finding the best conic approximation to the convolution curve of two compatible conics based on Hausdorff distance. *Comp. Aided Desi.*, 41:513–524, 2009.

[19] E. Jou and W. Han. Minimal energy splines with various end constraints. In H. Hagen, editor, *Curve and Surface Design*, pages 23–40. SIAM, 1992.

[20] T. Kim, Y. Kim, J. Suh, S. Zhang, and Z. Yang. Internal energy minimization in biarc interpolation. *I. J. Adv. Manu. Tech.*, 44:1164–1174, 2009.

[21] J. Malczak. Quadratic Bézier curve length. Undated web page; http://segfaultlabs.com/docs/quadratic-bezier-curve-length, accessed 2010.

[22] J. McCrae and K. Singh. Sketching piecewise clothoid curves. *Computers and Graphics*, 33:452–461, 2009.

[23] M. Moll and L. Kavraki. Path planning for deformable linear objects. *IEEE J. Robotics*, 22:625–636, 2006.

[24] J. R. Munkres. *Topology: A First Course*. Prentice-Hall, Upper Saddle River, NJ, 1975.

[25] J. Sanchez-Reyes. Complex rational Bézier curves. *Computer Aided Geometric Design*, 26:865–876, 2009.

[26] Z. Šír, B. Bastl, and M. Lávička. Hermite interpolation by hypocycloids and epicycloids with rational offsets. *Comp. Aided Geom. Desi.*, 27:405–417, 2010.

[27] D. J. Walton and D. S. Meek. A planar cubic Bézier spiral. *J. Comp. Appl. Math.*, 72:85–100, 1996.

[28] D. J. Walton and D. S. Meek. A Pythagorean hodograph quintic spiral. *Comp. Aided Desi.*, 28:943–950, 1996.

[29] D. J. Walton and D. S. Meek. Planar G^2 transition between two circles with a fair cubic Bézier curve. *Comp. Aided Desi.*, 31:857–866, 1999.

[30] D. J. Walton and D. S. Meek. Planar G^2 transition with a fair Pythagorean hodograph quintic curve. *J. Comp. Appl. Math.*, 138:109–126, 2002.

[31] S. H. Yahaya, J. M. Ali, and T.A. Abdullah. Parametric transition as a spiral curve and its application in spur gear tooth with fea. *Engineering and Technology*, 44:395–401, 2010.

[32] J. Yong and F. Cheng. Geometric Hermite curves with minimum strain energy. *Comp. Aided Geom. Desi.*, 21:281–301, 2004.